Frequency-dependent seismic anisotropy and its implication for estimating fracture size in low porosity reservoirs

Enru Liu, Sonja Maultzsch, Mark Chapman, and Xiang Yang Li, Edinburgh Anisotropy Project, Edinburgh, U.K.
John H. Queen, ConocoPhillips, Houston, Texas, U.S.
Zhongjie Zhang, Institute of Geology & Geophysics, Chinese Academy of Sciences, Beijing, China

The use of seismic anisotropy for characterizing subsurface fracture orientations and intensity has become increasingly popular. However, the reluctance of reservoir engineers to accept seismic anisotropy as a routine technique for fracture characterization is partly because of its inability to provide information about sizes and volume of fractures. Although both grain-scale micro-cracks and formation-scale macro-fractures are considered causes of seismic anisotropy, reservoir engineers are more interested in the latter as permeability in many hydrocarbon reservoirs is believed to be dominated by formation-scale fluid units (on the order of meters). We intend to fill this gap by developing new practical applications of seismic anisotropy including new theoretical models and new analysis methods.

Frequency-dependent anisotropy has been observed and can be explained by two mechanisms: seismic scattering by heterogeneities and fluid flow in fractured porous rock. In this article, we present a synthetic study demonstrating the dependence of seismic anisotropy on fracture sizes using a newly proposed multiscale fracture model. We then use this model to invert fracture sizes from field multicomponent shear-wave VSP data acquired in Bluebell-Altamonta, Utah. Our study has indicated a great potential of fracture size estimation in low porosity fractured reservoir, and thus we may potentially go beyond the conventional application of seismic anisotropy to predict fracture sizes and fracture volumes.

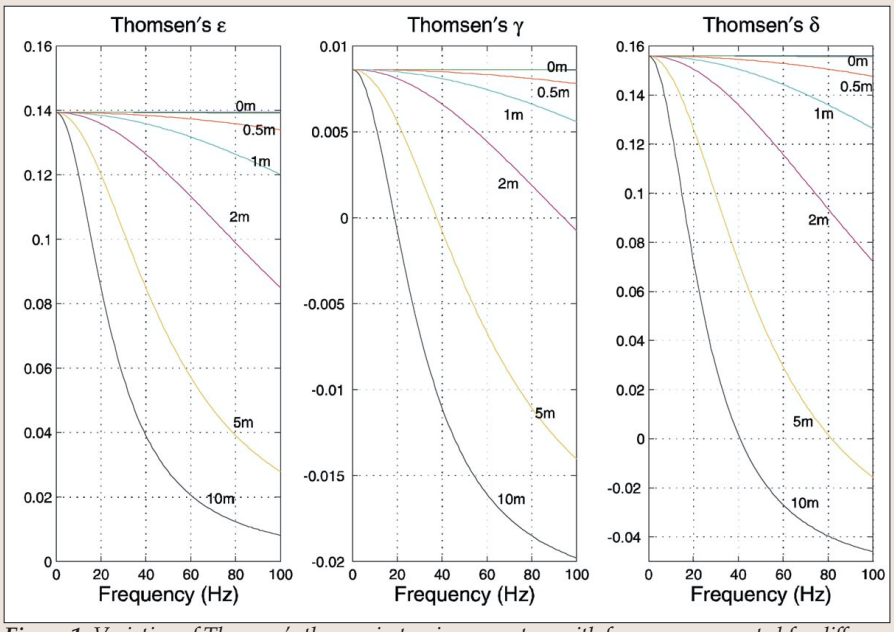

Figure 1. Variation of Thomsen's three anisotropic parameters with frequency computed for different fracture sizes (see text for parameters used).

Multiscale fracture model. The two most popular models for describing the elastic properties of fractured media are the so-called Thomsen's equant porosity model, and Hudson's thin-crack model. Thomsen's model assumes perfect fluid pressure equalization between the cracks and the surrounding rock, whereas Hudson's model assumes that the cracks are isolated with respect to fluid flow. Both models predict frequency independent behavior. In both models the magnitude of anisotropy is related to the fracture density, although the precise dependence is different in each case. This fracture density is defined as $\varepsilon=Na^3$ where N is the number of fractures per unit volume and a is the fracture radius. Unfortunately, radically different fracture distributions can have the same fracture density. This is because a few large fractures can give the same crack density as many smaller cracks.

If we are constrained to work with these two models, we can only obtain crack density and orientation from seismic data. To obtain information about fracture size, which can be critical for permeability prediction, a different model is required. Recently a new multiscale fracture model has been proposed by Chapman (2003). In contrast to the previous single scale models, the new model considers fluid interactions at two scales: mesoscale fractures inserted into a background porous rock with microcracks. The fracture lengths can be much larger than grain-scale pores or micro-cracks but are less than the seismic wavelength. The model introduces a characteristic scale length associated with meso-scale fractures which can play an important role at seismic frequencies. We briefly summarize this model below.

In porous rock with multiscale fractures, the effective elastic stiffness tensor is written as $C = C_0 - \phi C_1 - e_c C_2 - e_f C_3$, where ϕ is the porosity of the matrix, e_c is the microcrack density, and e_f is the macrofracture density. C_0 is the elastic stiffness of the matrix, C_1, C_2, and C_3 are the contributions of pores, cracks, and fractures, respectively. The size-dependent terms of elastic stiffness are linked by the relationship between two relaxation time scales, τ_m and τ_f, i.e.

$$\tau_f = \left(\frac{a_f}{a_m}\right)\tau_m ,$$

where τ_m is related to the standard microstructural squirt flow and τ_f is related to the mesoscale flow due to the presence of fractures. a_f is the fracture radius, and a_m is the grain size (the size of pores and microcracks). Note that a_f can be much larger than a_m. The frequency-dependent parts are governed by two terms: $(1+i\omega\tau_f)^{-1}$, which is related to fluid flow into and out of fractures, and

$$\left(\frac{1+i\omega\gamma\tau_m}{1+i\omega\tau_m}\right)^{-1} ,$$

which is related to pore-scale flow (γ depends on the Poisson's ratio of the matrix and fluid compressibility).

In the absence of fractures the

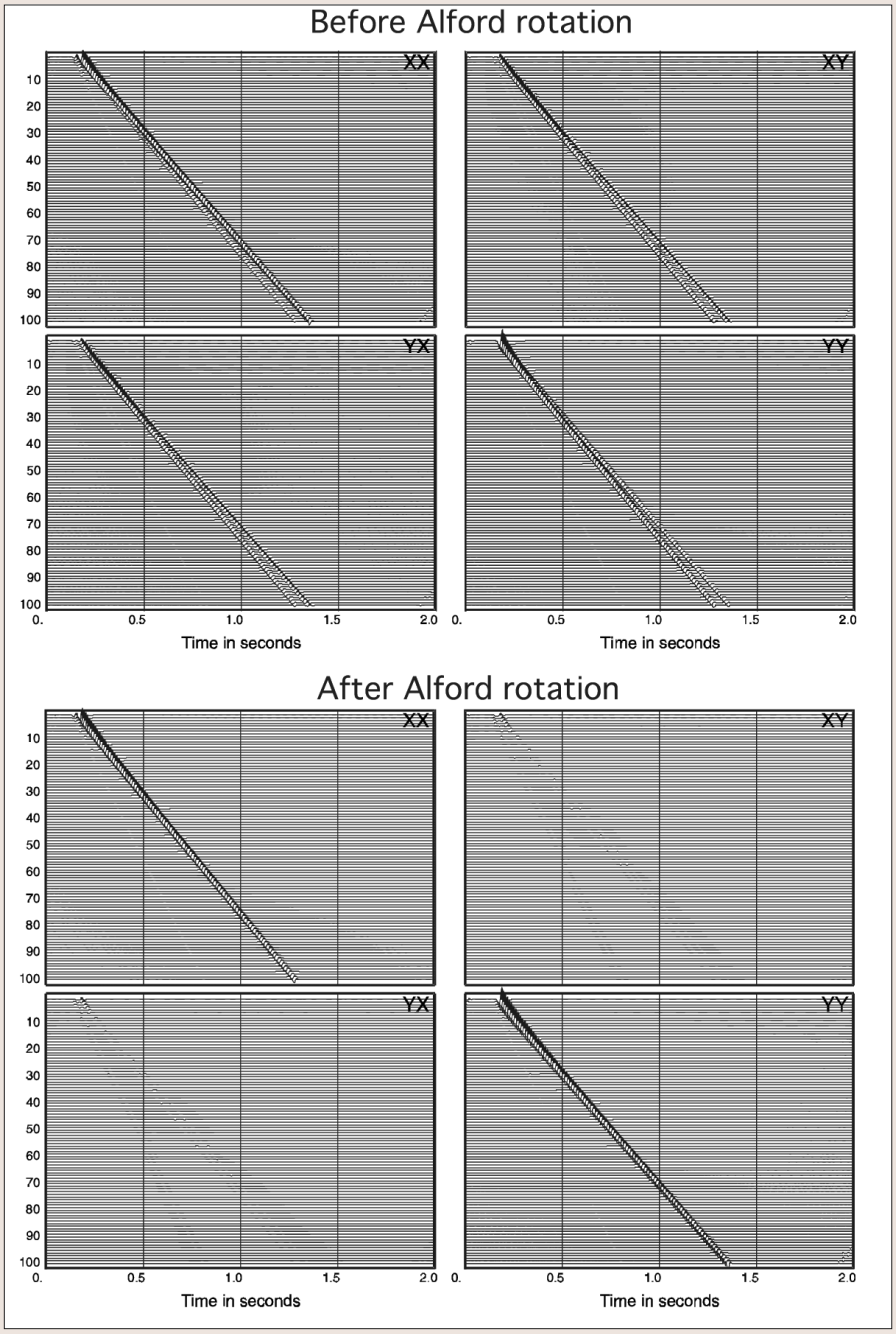

Figure 2. *Synthetic four-component shear-wave data (top) that have been rotated to the natural coordinates (bottom).*

model returns to the grain-scale squirt flow model. With the introduction of a fracture set, two characteristic frequencies exist: the traditional squirt flow frequency which can be estimated from laboratory data, together with a lower characteristic frequency which depends on the size of the fractures. A consequence of this is that propagation at seismic frequencies can be very different from that predicted in the low frequency limits, such as proposed by Thomsen (1995). It implies that dispersion can occur at seismic frequencies, or in other words seismic frequencies can no longer be safely regarded as the low-frequency limit. This model predicts frequency-dependent anisotropy, and an important example of this is the frequency dependence of shear-wave splitting which is sensitive to the fracture scale. Therefore we use this model to invert for fracture size.

Using simple algebra, we can obtain expressions of elastic stiffness in terms of Thomsen's parameters, or in terms of fracture compliance. Figure 1 shows the variation of the three anisotropic Thomsen parameters with frequency computed for different fracture sizes. The following rock properties have been used in our examples: V_P=3.5 km/s, V_S=2 km/s, ρ=2.3 g/cm^3, e_c=0.04, e_f=0.04, porosity ϕ =10%, and the relaxation time τ_m=10^{-7} (gas). The fracture sizes are indicated on each individual plot. We use f=30 Hz in all cases except where stated otherwise. That gives P- and S-wave wavelength of λ_P=116 m and λ_S= 66m, respectively. We can see that as the fracture size increases, or equivalently frequency increases, all three Thomsen parameters decrease, implying anisotropy decreases. When the size of aligned fractures is of the same order as the size of pores and micro cracks, there is little dependence of anisotropy parameters on frequency (i.e. the model reduces to the static or zero frequency equivalent medium theory).

Synthetic seismogram studies. We generate synthetic seismograms using an anisotropic Green's function and the complex elastic stiffness. The model is a VSP with an offset of 0.1 km and 100 receivers located at depths between 0.1 km and 2 km (spacing is 20 m). Two horizontal component sources that generate shear-waves are used and the source is a Ricker wavelet with a peak frequency of 30 Hz. The fractures have a length of 5 m, and are oriented 60° from the X-direction with a 10° dip. Conventional analysis of multicomponent shear-wave data involves simple rotation of horizontal four-component shear-wave data into the natural coordinate system through the use of standard methods such as Alford rotation to separate the two split shear-waves by minimizing the off-diagonal energy (Figure 2). The rotation angle then represents the polarization angle of the fast split shear-wave, which is interpreted as the fracture orientation. A cross-correlation can be applied to the fast and slow components to obtain the time-delays between the two split shear-waves. As expected, polarization angles do not show changes with fracture sizes. Figure 3 shows the polarization angles obtained for three models with different fracture lengths of 1 m, 5 m, and 10 m. Except for the shallow receivers, the polarizations are generally constant at 60°, which is very close to the direction of fracture orientation used in the models, and the small difference up to 2° is due to the 10° dip in the fracture orientation. Figure 4 shows the variations of time-delays between fast and slow shear-waves. We can immediately see that as receiver depth increases, time-delays increase linearly. More important for the purpose of the present study is the clear variation of time-delays with fracture length or frequency. As fracture size

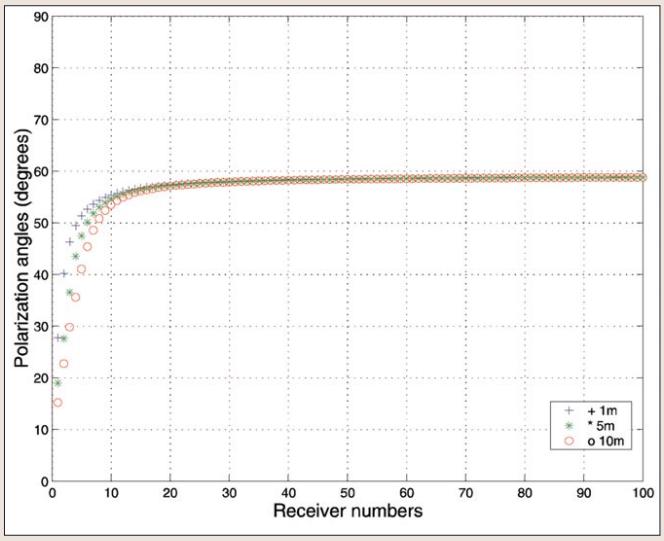

Figure 3. Variations of polarizations of fast split shear-waves with receiver numbers (depth) computed from synthetic four-component data for three different fracture sizes. The angles are relative to the in-line component.

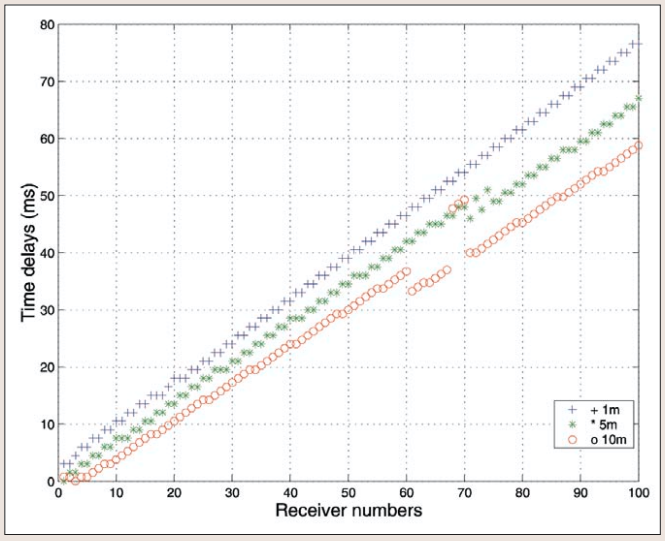

Figure 4. Variations of time-delays of split shear-waves with receiver numbers (depth) computed from synthetic four-component data for three different fracture sizes.

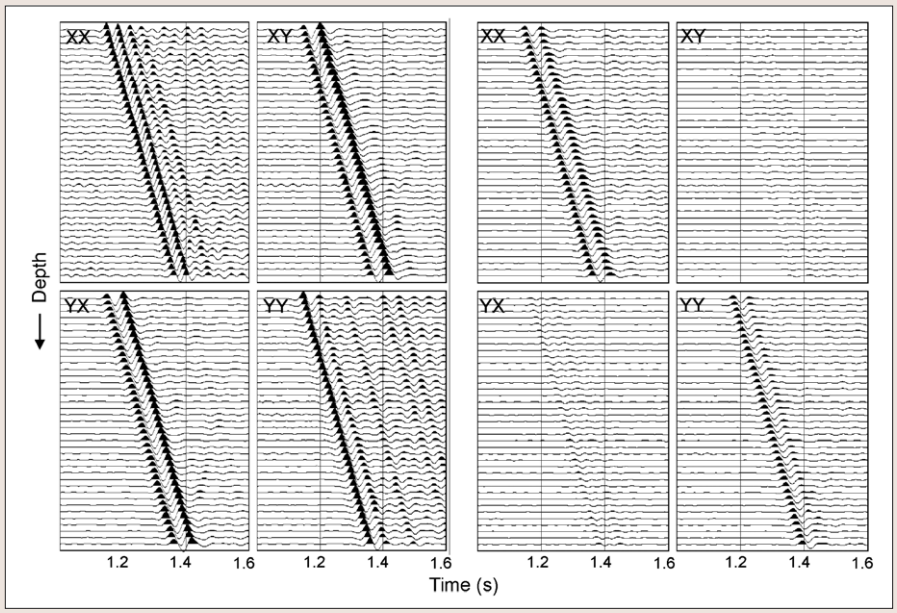

Figure 5. Bluebell-Altamont four-component shear-wave data (left) that have been rotated to the natural coordinates (right).

decreases or equivalently frequency increases, time-delay decreases.

Estimating fracture sizes from VSP data. We apply the model of Chapman (2003) to invert for fracture density and size from 9C VSP data from the Bluebell-Altamont field, Utah. The original and rotated VSP data are shown in Figure 5. Analysis of the data revealed a systematic decrease in time-delay between the split shear-waves with frequency. Figure 6 shows the computed relative error between observed and predicted time-delay versus frequency over a large range of fracture densities and sizes. We can see that there is a well-defined minimum around a fracture radius of about 3 m and a fracture density of 0.04, where the error is less than 5%. The plot also demonstrates that there are considerable differences in estimated fracture density between a high frequency model (Hudson's model) (upper end of the figure) and a low frequency model (e.g. Thomsen's model) porosity model (lower end of the figure). Figure 7 displays the time-delays obtained for each frequency range from the synthetic data (solid lines). For comparison, the dashed lines in Figure 7 show the time-delays found in the real data. The modeling results show very good agreement with the real data. In general the slopes of the lines corresponding to the synthetic data are slightly lower and the error appears to be higher at low frequencies. However, in terms of the parameter of interest, the fracture radius, the error in the results only corresponds to a change of about 20 cm, which is not significant. The estimated fracture size matches observations from cores and FMI logs very well.

Summary. Multiscale fluid interaction resulting in frequency-dependent anisotropy is a very interesting phenomenon. We argue that both scattering and fluid-flow may contribute to observed frequency-dependent anisotropy. However, we suggest that mesoscale fractures in porous rocks are more likely to be the dominant cause, at least in fractured hydrocarbon reservoirs. Our study has an important implication for characterization of natural fractures in that fracture sizes, which control the fluid flow, may potentially be predicted from seismic anisotropic measurements (note that meter-scale fractures are normally regarded as fluid flow units by reservoir engineers). In other words, we may potentially go beyond the static equivalent medium theories to extract information about fracture sizes and fluid properties in addition to fracture orientation and fracture density. We have presented results demonstrating the dependence of seismic anisotropic parameters on frequency. We have shown synthetic seismograms using far-field analytic expressions of the Green's function in anisotropic media. We emphasize the wave dispersion at low frequency, and have therefore restricted ourselves to seismic frequency bands in all examples. Our

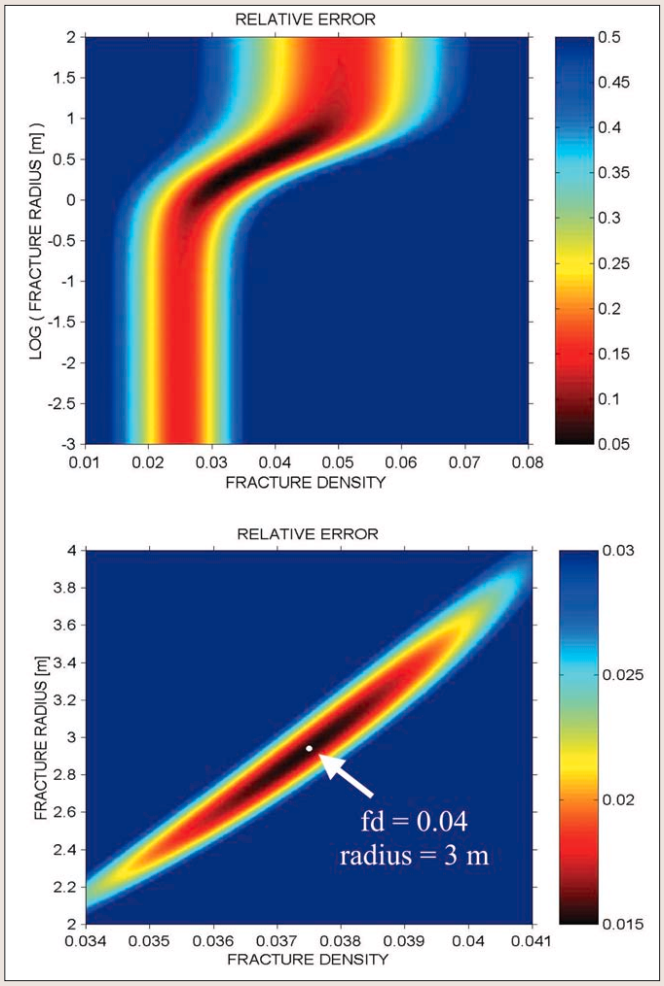

Figure 6. (Top) Rms error between predicted and measured time-delay/depth, evaluated over four frequency values for a range of fracture densities and sizes. (Bottom) The rms error zoomed around the minimum, where we can see that the error is less than 5%.

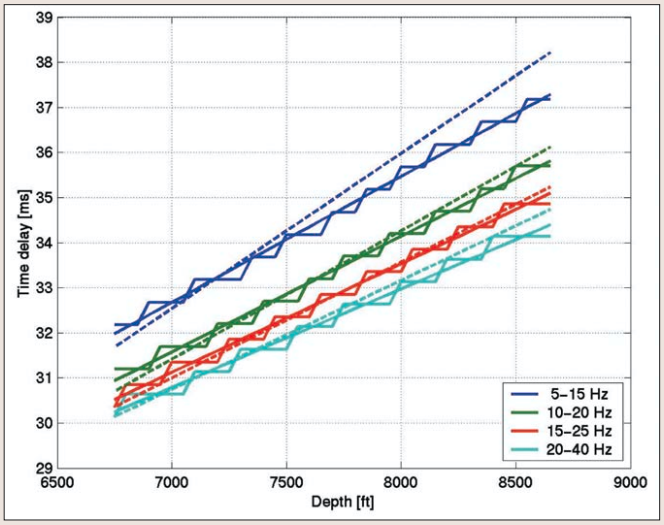

Figure 7. Time-delays estimated from the synthetic data for each frequency band (solid lines) in comparison with the results from the real data (dashed lines). The modeling results match the real data well. The errors are not significant in terms of the estimated values of fracture density and radius. The cause for the slight discrepancy will be a matter of future investigation.

results can explain observed variation of shear-wave anisotropy with frequency in terms of multiscale fluid flow in fractured porous rock. Synthetic seismograms and modeling of real VSP data reveal the variation of time-delays between split shear-waves with fracture size, and that as fracture length increases or frequency increases, shear-wave anisotropy decreases. Our study has indicated the great potential of using anisotropy measurements to estimate the fracture sizes, which are ultimately needed in reservoir simulation.

Suggested reading. Processing of multicomponent shear-wave data using Alford rotation can be found in "Shear data in the presence of azimuthal anisotropy, Dilley, Texas" by Alford (*SEG Expanded Abstracts*, 1986). Details of Hudson's microcrack can be found in "Wave speeds and attenuation of elastic waves in material containing cracks" by Hudson (*Geophysical Journal of the Royal Astronomical Society*, 1981, see also papers published by Pointer et al. in *Geophysical Journal International*, 2000). Thomsen's equant porosity model is in "Elastic anisotropy due to aligned cracks in porous rock" by Thomsen (*Geophysical Prospecting*, 1995). The multiscale fracture model used in this paper is in "Frequency dependent anisotropy due to mesoscale fractures in the presence of equant porosity" by Chapman (*Geophysical Prospecting*, 2003); a discussion about some of the implications of this model is in "10IWSA Proceedings" (*Journal of Applied Geophysics*, 2003). Details of field VSP data processing and acquisition parameters are in "P-wave and S-wave azimuthal anisotropy at a naturally fractured gas reservoir, Bluebell-Altamont Field, Utah" by Lynn et al. (GEOPHYSICS, 1999; see also her report to DOE in 1995, where frequency-dependent anisotropy was first reported) and "Observation and analysis of frequency-dependent anisotropy from a multicomponent VSP at Bluebell-Altamont Field, Utah" by Liu et al. (*Journal of Applied Geophysics*, 2003). Frequency-dependent anisotropy has also been observed in earthquake data, see papers "Frequency-dependent anisotropy due to fluid flow in bed-limited cracks" by Tod and Liu (*Geophysical Research Letters*, 2002) and "Frequency-band dependence of S-wave splitting in China mainland and its implications" by Liu et al. (*Science in China - Series D*, 2001). TLE

Acknowledgments: We thank Heloise Lynn for letting us use the VSP data from Bluebell-Altamont, and our colleagues Evgeni Chesnokov, John Hudson, Simon Tod, Kurt Nihei and Seiji Nakagawa for many useful discussions. We also thank the guest editor, Wenjie Dong, for his comments and many useful discussions during and after the carbonate workshop at SEG 2002. This work was supported by the Natural Environment Research Council (UK) through project GST22305, and sponsors of the Edinburgh Anisotropy Project (EAP), and is published with the approval of the Executive Director of the British Geological Survey (NERC) and EAP sponsors: Agip, BG, BP, ChevronTexaco, CNPC, ConocoPhillips, Kerr-McGee, Landmark, Marathon, Norsk Hydro, PGS, Schlumberger, TotalFinaElf, TradePartners UK/RIPED-LangFang, Veritas DGC.

Corresponding author: eliu@bgs.ac.uk